Acetylated cashew gum-based nanoparticles for the incorporation of alkaloid epiisopiloturine

Jessica do Amaral Rodrigues
Alyne Rodrigues de Araújo
Nadia Aline Pitombeira
Alexandra Plácido
Miguel Peixoto de Almeida
Leiz Maria Costa Veras
Cristina Delerue-Matos
Filipe Camargo Dalmatti Alves Lima
Augusto Batagin Neto
Regina Célia Monteiro de Paula
Judith Pessoa Andrade Feitosa
Peter Eaton
José Roberto Souza A. Leite
Durcilene Alves da Silva

Abstract

The natural alkaloid epiisopiloturine has recently become the focus of study for various medicinal properties, particularly for its anti-inflammatory and antischistosomal effect. The incorporation of active molecules in natural polymeric matrices has garnered increasing interest during recent decades. A new derivative of cashew gum successfully obtained by gum acetylation has shown great potential as a carrier in controlled drug release systems. In this work, epiisopiloturine was encapsulated in acetylated cashew gum nanoparticles in order to increase solubility and allow slow release, whereas the morphology results were supported by computer simulations. The particles were

produced under a variety of conditions, and thoroughly characterized using light scattering and microscopic techniques. The particles were spherical and highly stable in solution, and showed drug incorporation at high levels, up to 55% efficiency. Using a dialysis-based in vitro assay, these particles were shown to release the drug via a Fickian diffusion mechanism, leading to gradual drug release over approximately 6 h. These nanoparticles show potential for the use as drug delivery system, while studies on their potential anti-inflammatory action, as well as toxicity and efficacy assays would need to be performed in the future to confirm their suitability as drug delivery candidates.

Chemical compounds studied in this article

Sodium hydroxide (PubChem CID: 14798)
Formamide (PubChem CID: 713)
Pyridine (PubChem CID: 1049)
Acetic anhydride (PubChem CID: 7918)
Acetone (PubChem CID: 180)
Hydrochloric acid (PubChem CID: 313)

Keywords

Acetylation
Alkaloid
Cashew gum

1. Introduction

Natural products are widely used in the production of biomaterials. The abundant availability, lower toxicity rate, greater biocompatibility, and low costs of natural product make them promising sources of products of therapeutic interest [1].

The potential for biopharmaceutical applications of medicinal plants including their constituent compounds such as alkaloids, flavonoids, triterpenes and polysaccharides are the target of much research with several promising activities confirmed through pre-clinical trials reported in the literature [2].

Polysaccharides are natural macromolecules, one of the main constituents of plants composing the majority of the cell wall, providing structural support to these plants [3]. Cashew gum is a polysaccharide extracted from the *Anacardium occidentale* L. species, which are tropical plants extensively cultivated in Northeast Brazil. Cashew gum's structure is mainly composed of galactose, glucose, arabinose, and rhamnose groups, as well as glucuronic acid [4]. Some biological activities have been reported, including antimicrobial effects [5], antidiarrheal [6], anti-inflammatory [7], and gastroprotective effects [8]. More recently, its acetylated derivative (acetylated cashew gum) was used for preparation of polymeric nanoparticles to incorporate bioactive substances [9,10].

Alkaloids have attracted great attention for their ability to act as biological response modifiers. A wide range of biological activities of alkaloids have been reported, such as anti-inflammatory activity [11], antioxidant effects [12], antimicrobial action [13], analgesic effects [14] and as an antidepressant [15].

Epiisopiloturine (EPI) is an imidazole alkaloid extracted from *Pilocarpus* microphyllus, with in vitro and in vivo activity against *Schistosoma mansoni* [16]. Moreover, this alkaloid showed potent anti-inflammatory and antinociceptive activity, which might help combat the granuloma and inflammatory reaction caused by *S. mansoni* eggs [17]. Recently it was also proposed that EPI represents an attractive new treatment strategy for the prevention of NSAID-induced gastrointestinal lesions [18].

However, this promising alkaloid has low solubility in water, which can cause problems for its pharmaceutical bioavailability in biological systems. A first attempt at nanotechnological formulation was performed with liposomes, and there was a decrease in the cytotoxic effects in mammalian cells. The anthelmintic activity was slightly decreased when the drug was encapsulated in this way [19]. However, despite the good results, liposome formulations have a high cost.

Incorporation of active molecules in polysaccharide-based nanoparticles has become the subject of increasing interest during recent decades [20]. Nanoparticles made from natural polymers such as chitosan and gums have been used extensively for the controlled releasing of bioactive substances. Growing interest has been focused on nanoparticles obtained by self-assembly from hydrophobic polymers due to possible biomedical applications in many areas in the medical and pharmaceutical fields [21].

The aim of this study was to use two natural products, EPI and acetylated cashew gum (ACG) (Fig. 1) for nanoparticle formulation in order to improve the solubility of the alkaloid and enable controlled release, thus increasing the therapeutic benefit.

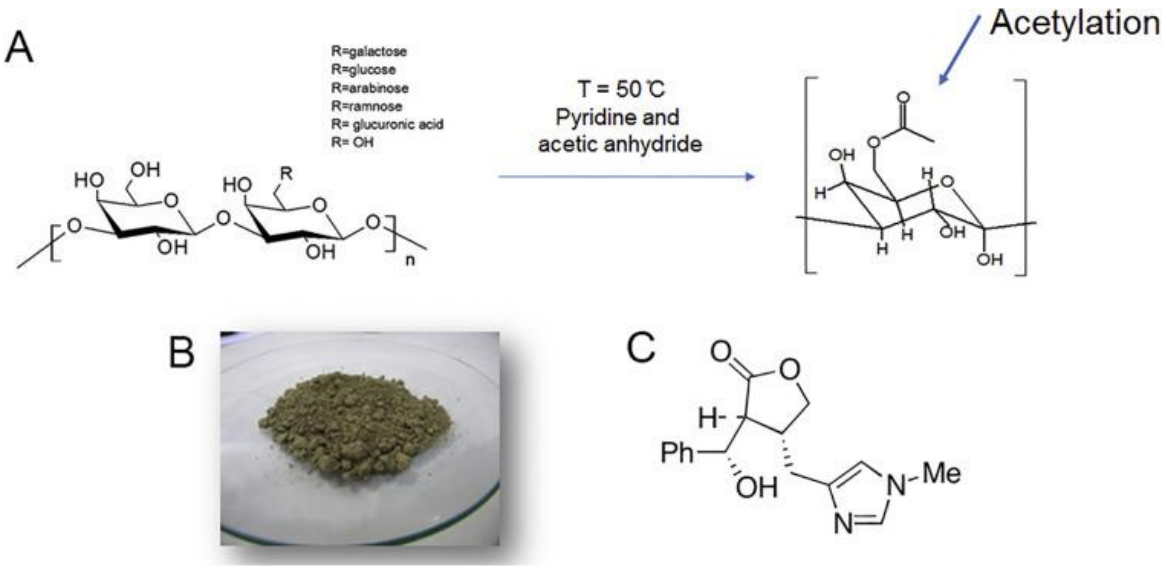

Fig. 1. Generalized chemical structure of acetylated cashew gum represented by the main constituent, galactose E (A), Industrial waste from the production of pilocarpine from leaves of *Pilocarpus* microphyllus (Jaborandi), from which the alkaloid epiisopiloturine is isolated (B), and epiisopiloturine alkaloid structure (C).

2. Materials and methods

2.1. Materials

The industrial residue obtained from jaborandi leaves for later purification were supplied by Anidro do Brasil Extractions S.A., Piaui Brazil. The alkaloid EPI (99.7% purity) were isolated by the method described by [16,17] from the waste obtained during the isolation of pilocarpine from *P. microphyllus*, a commercial product (Fig. 1B and 1C). Cashew gum used in the acetylation reaction has molar mass, obtained by size exclusion chromatography of 6.9×10^4 g/mol and the molar sugar content (%) for galactose; glucose; arabinose; rhamnose and glucuronic acid of 71.9; 14.4; 5.8; 3.6 and 4.3% respectively. The ACG was synthesized as described by Pitombeira et al. [9] with a degree of substitution of 2.8. All other reagents were of analytical grade.

2.2. Nanoparticle preparation

Nanoparticles were synthesized by a dialysis technique [9,22,23]. The gum was dissolved in dimethylsulfoxide at two different concentrations (0.05% and 0.1% w/w) and three gum/EPI proportions (by weight) were studied (10:1, 5:1 and 2:1). A solution of ACG (20 mL) was dialyzed against deionized water using a cellulose acetate membrane, molecular weight 14 kDa, during 24 h. Identical procedures were conducted for the synthesis of nanoparticles (NPs) with and without the EPI, totaling eight formulations designated of NP1 to NP8 as descripting on Table 1. The conductivity was used to monitor the water exchange. The resulting suspensions were then lyophilized and weighted.

Table 1. Size, particle concentration as prepared, polydispersity index (PDI), zeta potential (ZP) (mean), incorporated quantity drug load (IQ), and incorporation efficiency (IE), of nanoparticles prepared using different polysaccharide concentrations and polysaccharide to drug ratios.

Sample	ACG (%)	ACG:EPI	Size[a] (nm)	Particle concentration[a] (particles/mL)	Size[b] (nm)	PDI	ZP (mv)	IQ (%)	IE (%)
NP 1	0.05	–	126.0 ± 4.5	1.6×10^9	133.7 ± 0.9	0.148	−32.6 ± 0.2	–	–
NP 2		10:1	127.1 ± 6.1	1.1×10^9	132.0 ± 3.0	0.140	−26.7 ± 0.1	5.4 ± 0.5	59.8
NP 3		5:1	148.6 ± 3.5	1.3×10^9	107.4 ± 2.7	0.320*	−20.0 ± 0.1	8.8 ± 0.3	52.9
NP 4		2:1	129.1 ± 3.7	9.8×10^8	108.6 ± 0.7	0.226*	−17.4 ± 0.2	16.0 ± 0.2	48.1
NP 5	0.10	–	135.5 ± 2.1	4.7×10^8	155.1 ± 2.0	0.153	−26.9 ± 0.3	–	–
NP 6		10:1	132.6 ± 7.2	8.4×10^8	154.4 ± 1.5	0.120	−30.6 ± 0.2	6.9 ± 0.2	76.6
NP 7		5:1	101.6 ± 4.8	4.06×10^8	142.7 ± 0.9	0.175*	−23.1 ± 0.2	10.2 ± 0.3	61.2
NP 8		2:1	165.6 ± 5.3	2.6×10^8	126.2 ± 1.9	0.212*	−25.1 ± 0.1	10.7 ± 0.1	32.2

2.3. Nanoparticle characterization

The average hydrodynamic diameter and polydispersity index (PDI) were determined by means of dynamic light scattering analysis spectroscopy (photon correlation — DLS) and nanoparticle tracking analysis (NTA). The DLS used a laser wavelength of 633 nm at a fixed scattering angle 90 and the zeta potential was determined by electrophoretic mobility of the samples using Malvern Zetasizer Nano equipment, ZS Model 3600. Samples were measured in triplicate and the average values are reported here. The stability of the various EPI-ACG formulations was evaluated by determining the hydrodynamic diameter and PDI values of the nanoparticles with storage time. The samples were stored in Eppendorf tubes and kept at a temperature of 4 °C. The measurements were performed weekly for a period of weeks.

NTA was carried out using a NanoSight NS300 instrument with a 642 nm laser module and NTA 3.2 software, to obtain the diameter and concentration of particles suspended in the feed. An aliquot was taken using a plastic syringe and injected slowly into the sample chamber (approximately 1 mL). Five videos of 1 min length each were captured advancing the sample enough so that a previously unmeasured set of nanoparticles could be captured by the camera before starting each video. This allowed the measurement of a larger number of different particles across the aliquot. The analysis, namely the detection threshold, was set depending on the scattered light intensity observed in the captured videos. Each one of the videos was analyzed independently and the results are automatically merged into one particle size distribution chart.

The morphology of the nanoparticles was measured by Atomic Force Microscopy (AFM). To obtain the images a TT-AFM from AFM Workshop microscope, operated in vibrating mode was used. We used NSG10 (NT-MDT) cantilevers with a resonant frequency of approximately 280 kHz. Samples of 5 μL of nanoparticle suspension were deposited on freshly cleaved mica. The immobilized samples were rinsed with water and then thoroughly dried before analysis. The images were analyzed using the software program Gwyddion 2.33.

2.4. Amount of drug incorporated and the incorporation efficiency (%IE)

After lyophilization the EPI loaded nanoparticles were dissolved in methanol with stirring for 1 h and then the absorbance at 258.3 nm was measured. The amount of EPI in the nanoparticles was determined by UV–Vis spectroscopy, measuring the absorbance at 258.3 nm. Amount of incorporated drug was calculated using a calibration curve to determine the relationship between the absorbance and the concentration using the concentration range of 0.05 to 1 mg/mL with methanol as solvent. The incorporated quantity (IQ) was determined by Eq. 1, and then the incorporation efficiency (IE) determined by Eq. 2 [22]:(1)

(2)

*The ACG mass in nanoparticle was calculated by NP mass minus EPI loaded mass.

2.5. In vitro release of EPI

The release profile was determined using a dialysis system. The nanoparticles (6 mg) were introduced into cellulose acetate membrane (molecular weight cut-off 14 kD) and dialyzed against 50 mL phosphate buffer pH 7.4 at 37 °C. Aliquots of 1 mL were collected at 30-minute intervals in the first 4 h and hourly in the next 6 h. The same amount of buffer was replaced upon each aliquot removal so that the volume remained constant. Absorbance measurements at UV–Vis spectroscopy were used to quantify the alkaloid released using a calibration curve previously established in the same medium used for the release test. The experiment was performed in triplicate and the drug concentrations were corrected considering the dilution factor.

2.6. Statistical analysis

Statistical analyses were performed by using one-way ANOVA and Tukey's test using Graphpad Prism. All data were expressed as the mean ± SD (standard deviation) of three independent experiments in the tables and figures. Statistical significance for this study was considered at $p < 0.05$.

2.7. Computational details

The cashew gum polymer was simulated by considering its major component, galactose E (see Fig. 1). Preliminary studies on the saturation of the electronic properties of the

oligomers as a function of the number of units was initially conducted [24]. Oligomeric systems with distinct units were designed with the aid of Molden computational package [25] and pre-optimized in a Hartree-Fock approach employing the Austin Model 1 (AM1) semi-empirical Hamiltonian, implemented in MOPAC2016 computational package [26]. Based on the saturation analysis, a structure with 12 units has been chosen as the oligomeric model of AGC (AGC-n12). The chemical structure of EPI molecule was extracted from the crystallography database [27]. The molecule and oligomer geometries were fully optimized within the Kohn-Sham Density Functional Theory framework [28] (DFT), using the B3LYP exchange-correlation functional [29], and 6-31G basis set. The geometry optimizations were carried out with the aid of Gaussian 09 computational package [30].

Condensed-to-Atoms Fukui Indexes (CAFIs) [31] were evaluated to identify the position of reactive sites on the polymer and EPI molecule, and evaluate their interaction. Such indexes describe how the electronic populations of the atoms change after the releasing/withdrawing of electrons in/from a given system, allowing to identify molecular sites that are prone to interact with nucleophiles (f^+) or electrophiles (f^-) [31]. In particular, these descriptors have been successfully employed in the study of polymers [[32], [33], [34], [35]] and molecules reactivity [11,27,31,36,37]. The simulations were carried out in vacuo and without temperature effects using the same DFT/B3LYP/6-31G approach employed in the optimizations. Hirshfeld partition charge model was employed to estimate the electronic populations to avoid negative CAFIs [[31], [32], [33], [34], [35]].

3. Results and discussion

3.1. Nanoparticle characterization

EPI was incorporated into a polymeric matrix and polymeric nanoparticles obtained using acetylated cashew gum. The formation of nanoparticles was monitored by DLS and moderate polydispersity was found for all the samples (Supplementary Fig. 1). Table 1 shows the sizes of nanoparticle samples with and without EPI for two gum concentrations. Gaumet, Vargas, Gurny & Delie [38] emphasize the size of the nanoparticles as an essential feature in the biodistribution of the active ingredient. To produce the desired

therapeutic effect nanoparticles should exhibit a particle size consistent with the target organ.

Nanoparticles with size below 6 nm can pass through the fenestrations of the mucous membranes, tissue skeletal, cardiac, smooth muscle, and skin, while nanoparticles of 20 to 30 nm in size can reach the kidneys. Nanoparticles around 150 nm are able to penetrate the liver and spleen. The nanoparticles prepared in this study had a size distribution between 107 and 156 nm (hydrodynamic diameter obtained by DLS), which are favorable for administration of passive drugs, whereas nanoparticles with sizes <200 nm are able to resist attack by the reticulum endothelial system [39,40]. As EPI acts as a potent agent against schistosomiasis, the nanoparticles developed in this work may be very interesting for this alkaloid application in order to improve its biodistribution into the liver.

In polymeric nanoparticles that have been described in the literature, it is seen that with increasing polymer concentration in the preparation, there's generally an increase in particle diameter. Galindo-Rodriguez et al. [41] describe two reasons for this behavior. Firstly, upon increasing the amount of polymer, there is a greater number of polymer chains per volume of solvent, polymer-polymer interactions are favored, which leads to the formation of particles with larger sizes. Secondly, the increase in polymer concentration causes an increase in viscosity of the organic phase, providing greater resistance to mass transfer, such that the diffusion of the polymer from the organic phase to the aqueous phase is reduced and larger nanoparticles are formed. The incorporation of the alkaloid in polymer nanoparticles produced a significant reduction ($p < 0.001$) in the nanoparticle size. In this work, only for the ratio polymer to alkaloid of 10:1 (i.e., samples NP 2 and NP 6) was there no statistically significant change (Table 1).

Pitombeira et al. [9] describe synthesis of nanoparticles using acetylated cashew gum to incorporate indomethacin, and observed similar behavior. The average diameter of the drug-free nanoparticles was 179 nm while for those with the addition of the active ingredient 140 nm was found. Using the same polymeric matrix, Dias et al. incorporated diclofenac diethylammonium and also noted a reduction in the diameter of the incorporated nanoparticles compared to nanoparticles without the addition of the active ingredient [10]. In obtaining polymeric nanoparticles as drug delivery platforms, the need for affinity between the polymer used and the incorporated agent has been recognized as an important factor [42].

The PDI, which is a measure of the polydispersity in sizes, was found to be between 0.1 and 0.3 for all alkaloid proportions tested in this work. The zeta potential of the nanoparticles with and without EPI were all negative, ranging from −17.4 to −31.6 mV (Table 1). According to the literature, 30 mV in modulus or greater suggest good stability in suspension, since the surface charge reduces particle aggregation [43]. The zeta potential of nanoparticles is influenced mainly by the nature of the particle constituents [44]. In this case, the negative zeta potential is probably due to acetylated groups present in cashew gum structure.

For four formulations (NP 2, NP 3, NP 6, and NP 7), the incorporation efficiency (IE) exceeds 50%. A reduction in incorporation efficiency was observed, with increasing amount of the active component in the formulation. This behavior was also observed by Dias et al. [10], when the amount of drug added during the synthesis was increased. This result suggests that upon increasing the amount of alkaloid in the nanoparticle, a saturation concentration of the drug in the polymeric matrix was reached, reducing the amount of encapsulated drug [45].

There are several factors that can influence the proportion of drug associated with the polymer matrix in nanostructured systems, including the physical and chemical characteristics of the formulation, such as pH, viscosity, etc., polymer structure, active characteristics of the particle surface and the amount of drug added to the system [46].

Hornig, Bunjes & Heinze [47], using dialysis for the synthesis of polymeric nanoparticles, incorporated nonsteroidal anti-inflammatory drugs (ibuprofen and naproxen), and evaluated the influence of the degree of substitution of the polymer used (dextran) on the amount of drug incorporated. A 37 to 68.3% variation in the efficiency of the system was observed depending on the degree of substitution achieved.

The samples were also characterized by NTA. The histogram in Supplementary Fig. 2 shows a moderately polydisperse distribution, confirming the data obtained by DLS. In particular, the NTA seems to indicate that some of the polydispersity could be due to small aggregates in solution, while the main size peak for each sample was quite narrow. Additionally, it was observed that the amount of polymer in the formulation could alter the particle concentration obtained. Oliveira et al. [48] synthesize nanoparticles of

chitosan and note that interference does not occur in the concentration with the addition of the bioactive.

Comparing the results obtained by DLS and NTA, differences ranging from 3.8 to 38.8% in the particle sizes were observed. The DLS technique provides the average particle size by measuring fluctuations in the intensity of scattering and is commonly affected by the presence of a small number of large particles. Combination of DLS with NTA has been recommended as it provides additional information about the distribution of sizes in the samples [23,49].

3.2. Stability

Fig. 2 shows data on size (Fig. 2A) and PDI (Fig. 2B) as a function of storage time. The colloidal stability of the solutions can be affected by numerous factors such as the adsorption of surface-active molecules on the nanoparticle, the use of surfactant in the synthesis of particle, chemical composition of the polymer and the drug, and also premature release of the active component. Is it also important to assess the visual aspect of the solutions that could indicate that advanced aggregation has occurred [44]. The nanoparticles showed good physical and chemical stability and no macroscopic changes (creaming, sedimentation or flocculation) were observed during the study period.

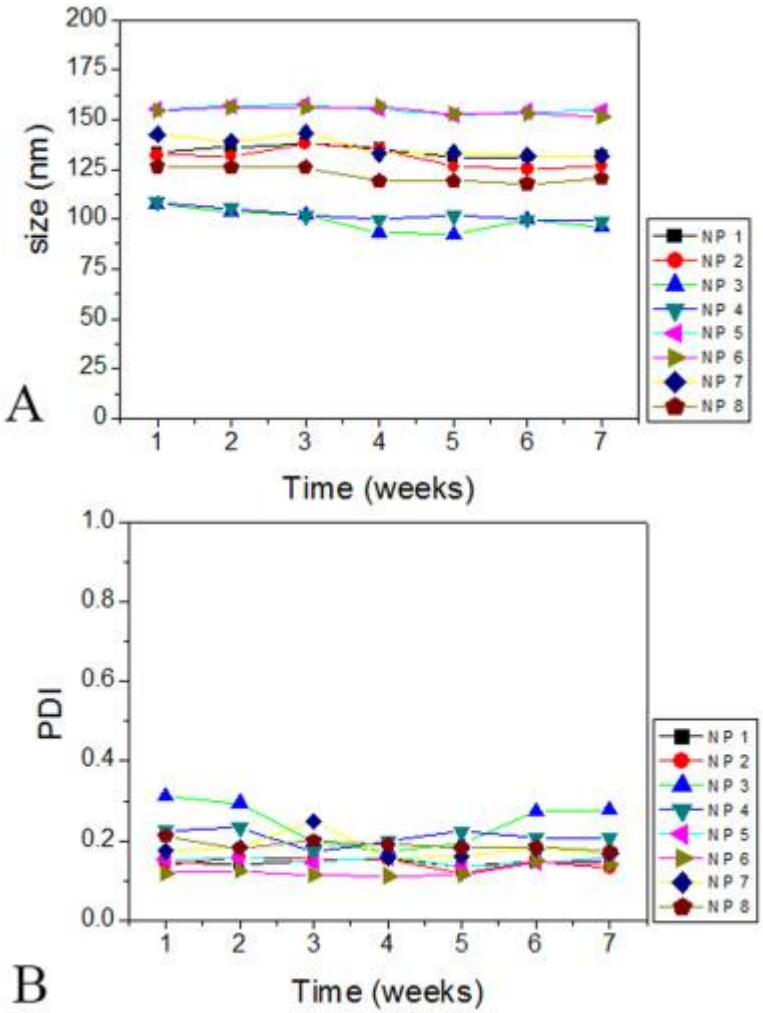

Fig. 2. Hydrodynamic diameter (A) and polydispersity index (PDI; B), both measured by DLS, measured as a function of storage time after synthesis.

As shown in Fig. 2A, there was very little particle size variation as a function of storage time (over 7 weeks) indicating good stability of the formulations. Regarding the PDI over time some greater variations in the proportions 5:1 (NP 3 and NP 7) for both polymer concentrations. However, they did not increase significantly, nor did they show any specific trend in PDI value. This could be due to some dynamic aggregation/deaggregation behavior, i.e. a reversible process, unlikely to affect medium-term storage. For the other drug to polymer ratios only mild changes in function of time were observed indicating good colloidal stability of these systems.

3.3. Morphology

The morphology aspects of representative nanoparticles (with and without EPI) obtained with AFM measurements are shown in Fig. 3. As representative samples, NP 1, NP 4, NP

5 and NP 8 were chosen. These represent the nanoparticles with no drug, and those with the most drugs, in the two gum concentrations tested. The nanoparticles surfaces were in general smooth, with no ridges. Kumar et al. [50] explain the lack of surface roughness in polymeric nanoparticles by the elastic nature of the polymer, which adapts to different shapes reducing conditions and possible surface imperfections. In general, the nanoparticles were globular, approximately spherical in shape. Those produced with the lower concentration had less spherical shape.

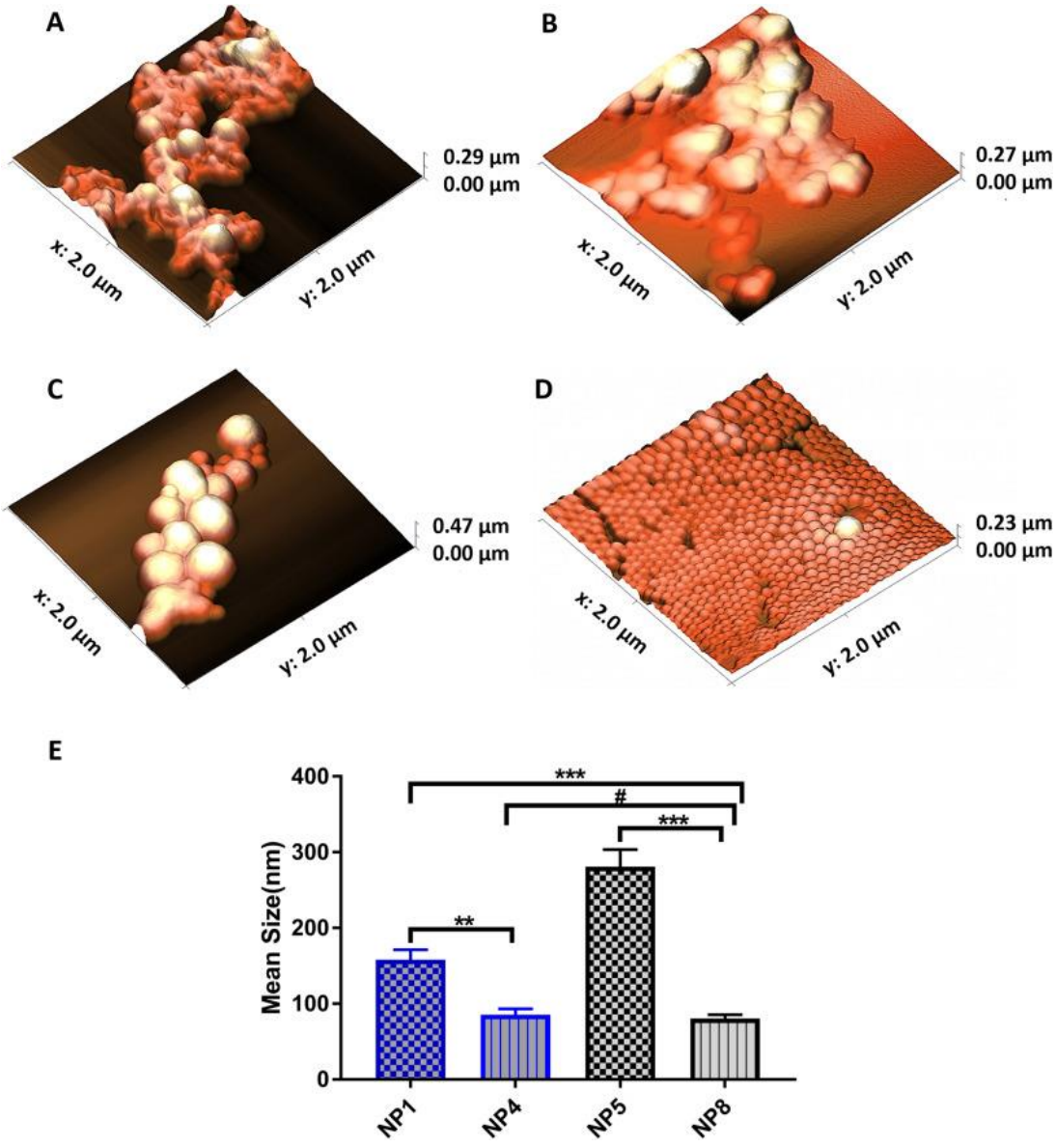

Fig. 3. AFM height images of nanoparticles prepared by dialysis. (A) NP 1; (B) NP 4; (C) NP 5; (D) NP 8; (E) size data from AFM analysis.

The drug-loaded particles produced with 0.05% acetylated cashew gum are the most irregular. While this result was seen in all the images obtained, it is not possible to rule

out that this was an effect of the drying of the nanoparticles before imaging. The mean size of the nanoparticles from AFM analysis were 158.1 ± 13.0, 85.5 ± 7.5, 280.7 ± 22.7 and 80.4 ± 5.0 for NP 1, NP 4, NP 5 and NP 8, respectively. Nanoparticles with EPI (NP 4 and NP 8) have similar size and are smaller than the NPs without EPI (NP 1 and NP 5). The smaller particles in the latter case may be due to the formation of a more hydrophobic core leading to particle contraction [9].

CAFIs analysis also supports the morphology results, as shown in Fig. 4 based on the saturation analysis, considering a gum structure with 12 units has been chosen and designated as AGC-n12. Blue colors indicate non-reactive sites, yellow, green and red indicate the increase of the local reactivity. Since f^+ and f^- indicate regions that are prone to interact with nucleophiles, and electrophiles, respectively, it is interesting to evaluate the AGC-n12 and EPI CAFIs as pairs: f^-(AGC-n12)./f^+(EPI), f^+(AGC-n12)/f^-(EPI).

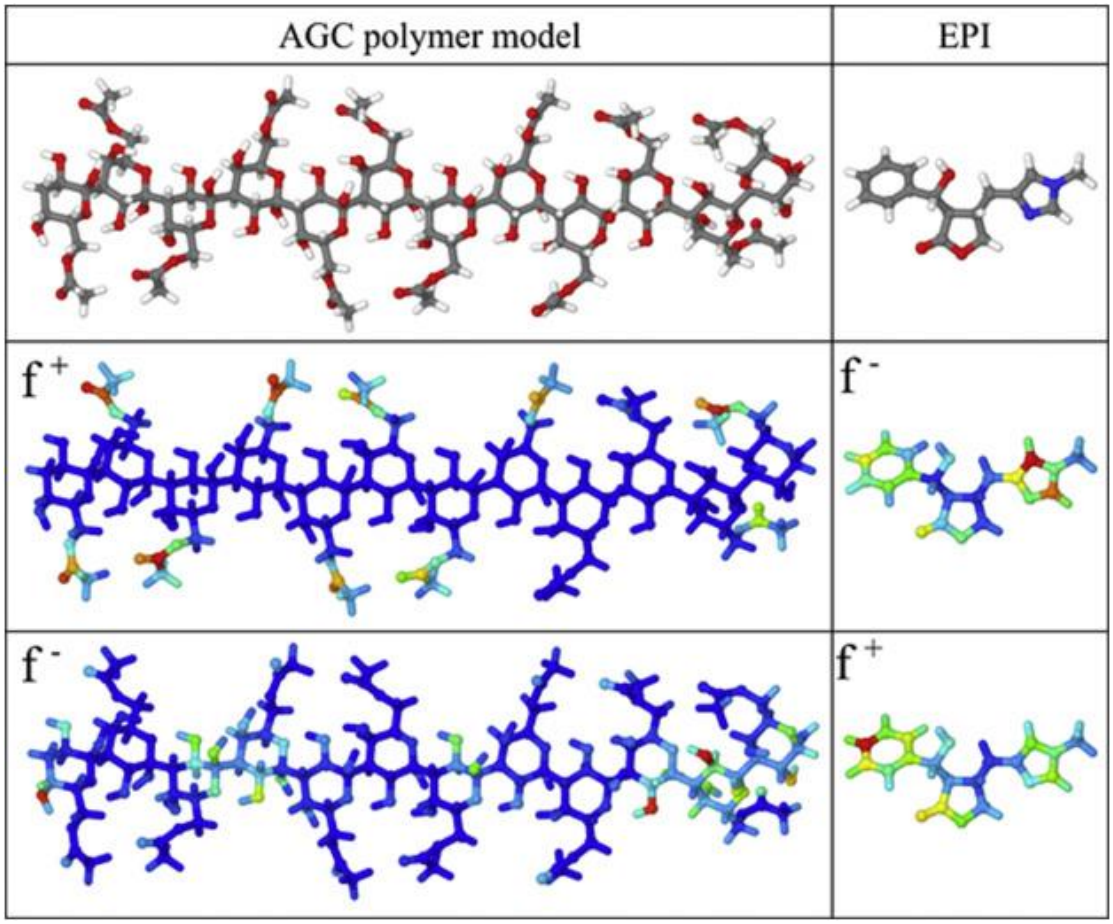

Fig. 4. Molecular 3D representation of the 12 units cashew gum (left) and the EPI (right). CAFIs results for the nucleophilic (f+), electrophilic (f−) and radical (f0) attacks, whereas the rainbow color scheme indicates low reactivity (purple) to high reactivity (red).

As can be noticed, the EPI molecule shows a remarkable activity, with well separated sites for reactions towards nucleophiles (para position of the phenyl) and electrophiles (imidazole group) located at more internal regions (protected carbons), which emphasize its hydrophobic behavior. On the other hand, the polymer presents higher reactivity at the side groups, especially on the oxygens, which facilitates an effective solvation of such material in water.

A comparative analysis of the f^{-}(AGC-n12)./f^{+}(EPI) and f^{+}(AGC-n12)/f^{-}(EPI) pairs suggests that EPI can interact efficiently with the polymer side chains, especially considering f^{+}(AGC-n12)/f^{-}(EPI), where imidazole interacts with the oxygen site atoms of the polymer. Given the spatial distribution of the reactive sites the alkaloid is not supposed to stain aligned with the polymer backbone, limiting the number of incorporated species, which is compatible with experimental results.

The above mentioned interaction between EPI and the oxygens of the AGC acetate groups, could lead to an effective reduction of the polymer hydrophilicity, which could explain the particle contractions observed after drug incorporation. It is important to note that the f^{-}(AGC-n12)./f^{+}(EPI) and f^{+}(AGC-n12)/f^{-}(EPI) interactions are not supposed to occur concomitantly due to the existence of steric effects, so AGC/EPI system still retain a hydrophilic core that allow its solubilization in water.

3.4. In vitro release of EPI

Therefore, based on the results obtained for particle size, yield and incorporated quantity drug load, the NP 8, nanoparticles produced by the dialysis method with an ACG:EPI ratio of 2:1 were chosen for the in vitro release. The drug release profile was analyzed by diffusion through a dialysis membrane in phosphate buffer. Fig. 5 shows the amount of alkaloid released versus time, wherein it can be seen that EPI has a slow and gradual release profile, with equilibration occurring after around 6 h release, which is also compatible with the hydrophobic interactions between the cashew gum and the EPI identified by DFT calculations and absence of reactive sites on the polymer backbone (Fig. 4). Numerous mathematical models of drug release were described in literature [[51], [52], [53]]. The Korsmeyer–Peppas model [53] was applied to the ACG-EPI systems. The model is based on the power law. In the equation, the exponent “n” is a parameter that varies according to the system geometry and determines the release

mechanism. If “n” is less than or equal to 0.5 the mechanism is said to be Fickian diffusion, while if it is between 0.5 and 1, non-Fickian diffusion is taking place [54].

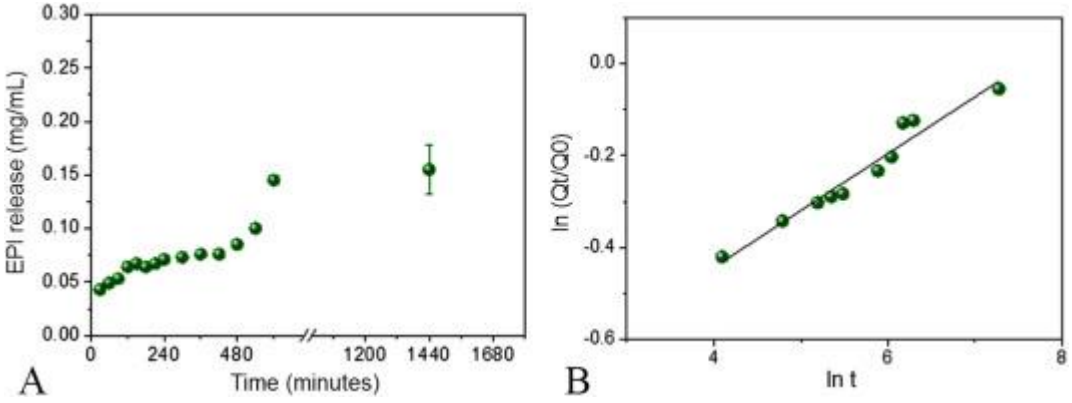

Fig. 5. In vitro drug release profile data from dialysis experiments for EPI from NP 8 nanoparticles. Data represents mean value of 3–4 replicates ± standard deviation (A). Mechanism associated with in vitro release of EPI from NP 8, according to the Korsmeyer–Peppas model ($n = 3$) (B).

The diffusion exponent (n) was obtained from the linear coefficient of the graph plotted in Fig. 4, showing ln Qt / Q_0 versus ln t in the first 600 min of the release alkaloid. In the graph, the slope and intercept of the plot gives the value of K and n. The value of “n” was found to be 0.37 for the release of EPI, suggesting that the mass transfer follows the Fickian diffusion model. According to Melo et al. [55], porous release systems may have values <0.5 because the process is a combination of the diffusion from the polymer matrix and the diffusion through the pores partially filled with water. This could corroborate the AFM results, where in some cases, collapse upon drying occurred for drug-containing particles. Pitombeira et al. [9] and Dias et al. [10] using the same polymeric matrix found “n” of 0.43 and 0.27, respectively, with the same release profile, corroborating the results found in this study.

4. Conclusion

Nanoparticles made with acetylated cashew gum were shown to be viable drug delivery vehicles, with the highly efficient incorporation of EPI. The nanoparticles produced showed moderate polydispersity, and were found to be stable over time. Details regarding the interaction of EPI molecules and AGC polymer model were investigated via DFT calculations. The release of this alkaloid drug took place of a period of hours, following typically Fickian diffusion mechanism. These nanoparticles show potential for the use as

drug delivery system, while studies on their potential anti-inflammatory action, as well as toxicity and efficacy assays would need to be performed in the future to confirm their suitability as drug delivery candidates.

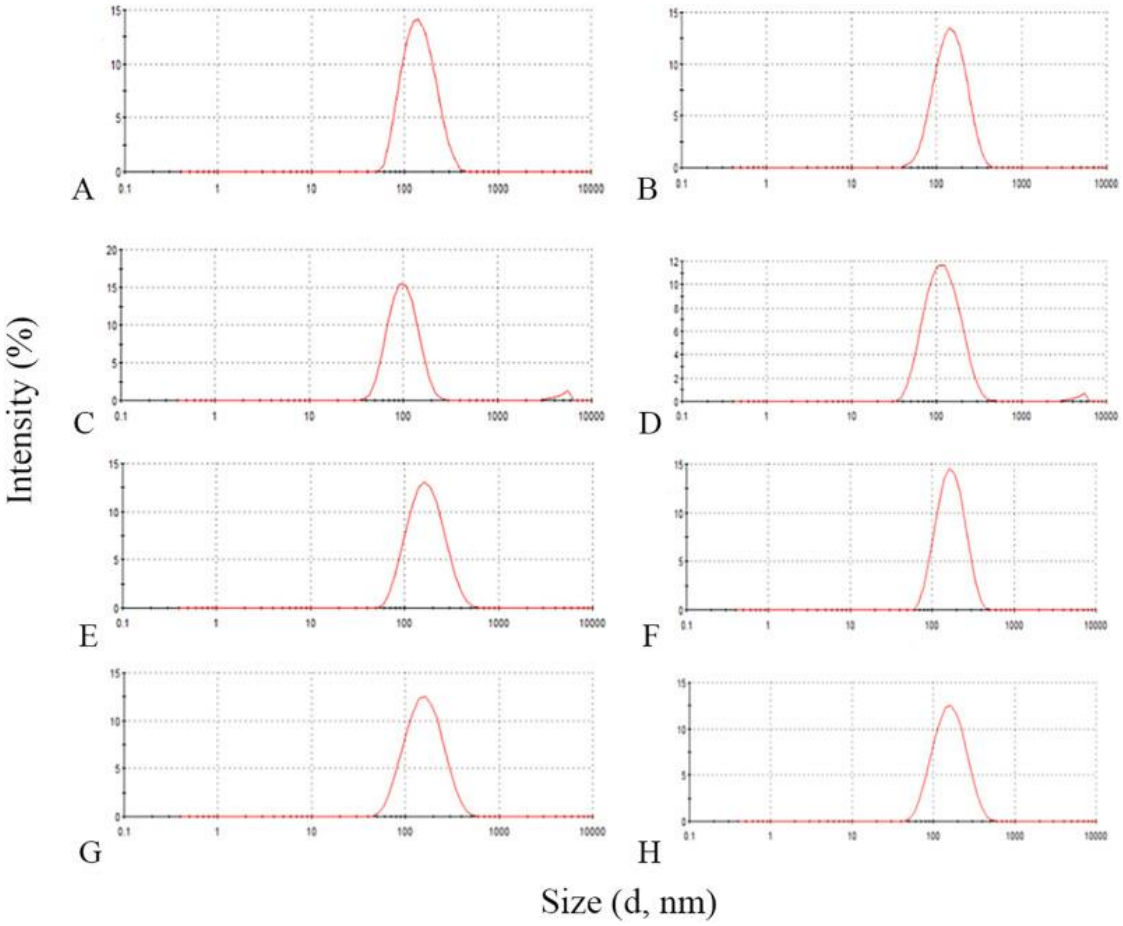

Supplementary Fig. 1. Size distribution data (intensity) from light scattering (DLS). (A) NP 1, (B) NP 2, (C) NP 3, (D) NP 4, (E) NP 5, (F)NP 6, (G) NP 7, and (H) NP 8.

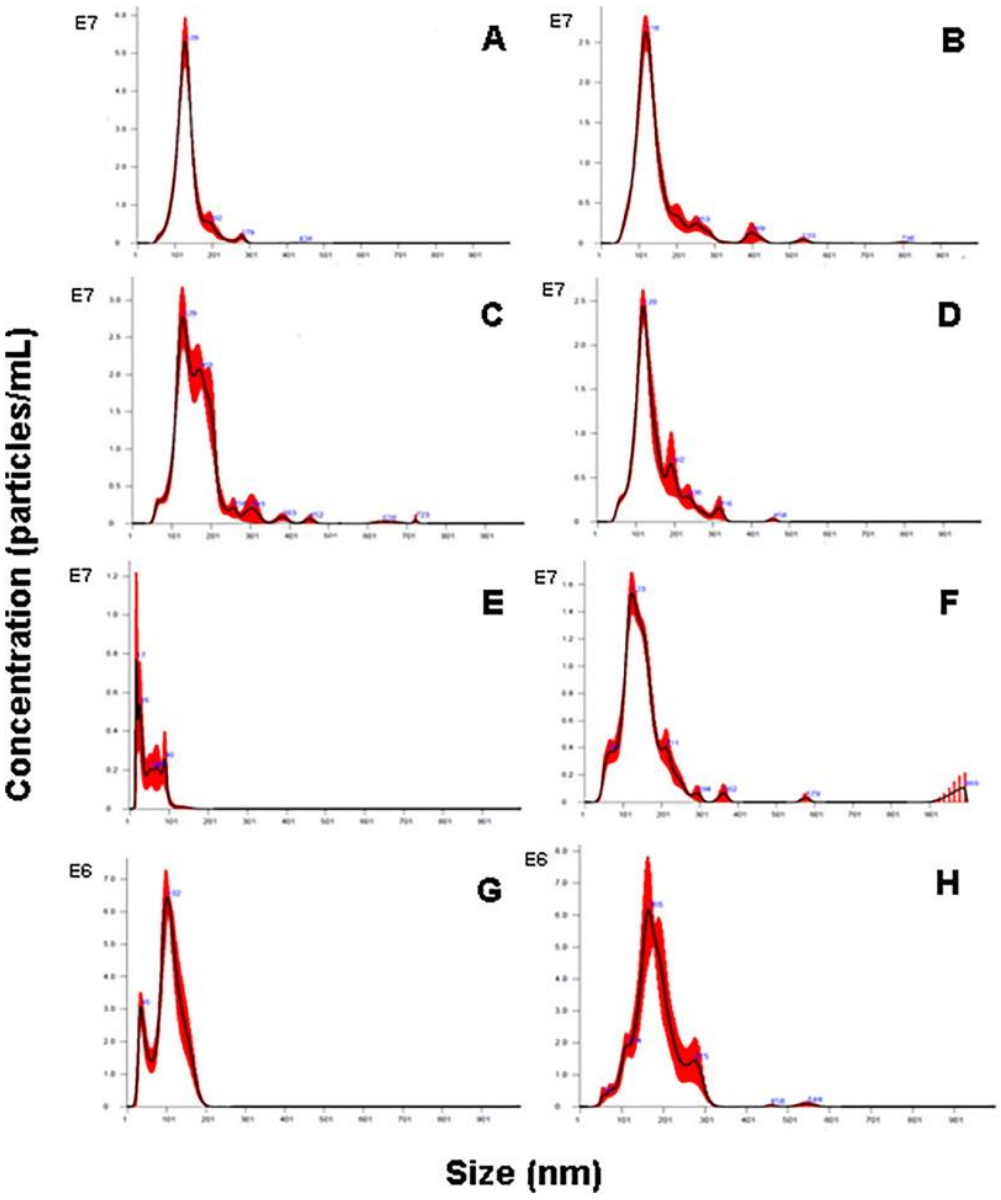

Supplementary Fig. 2. Quantitative particle size analysis by nanoparticle tracking analysis (NTA). Merged results for samples (A) NP 1 (Mode: 128.0 ± 4.5 nm) (B) NP 2 (Mode: 118.9 ± 6.1 nm), (C) NP 3 (Mode: 128.3 ± 3.5 nm), (D) NP 4 (Mode: 119.8 ± 3.7 nm). (E) NP 5 (Mode: 17.3 ± 2.1 nm;), (F) NP 6 (Mode: 123.4 ± 7.2 nm), (G) NP 7 (Mode: 101.6 ± 4.8 nm), (H) NP 8 (Mode: 165.3 ± 5.3 nm).

Acknowledgments

This work was conducted in partnership with the Polymer Laboratory of the Federal University of Ceará for polymer modification. The authors thanks Foundation for Science and Technology (FCT) for the fellowships SFRH/BD/97995/2013 (AP) and SFRH/BD/95983/2013 (MPA), in the context of the POCH program. The work at UCIBIO/REQUIMTE was supported by FCT through project UID/MULTI/04378/2013 – POCI/01/0145/FEDER/007728 with financial support from FCT/MCTES through

national funds and co-financed by FEDER, under the Partnership Agreement PT2020. The work at REQUIMTE/LAQV received financial support from the European Union (FEDER funds through COMPETE) and National Funds (FCT) through project UID/QUI/50006/2013. The computational time was provided by GRID-Unesp, SICC/IFSP and CENAPAD/SP. The authors also acknowledge CNPq and CAPES for a scholarship and financial aid.

References

[1]

A.C. Pinto, D.H.S. Silva, V. da S. Bolzani, N.P. Lopes, R. de A. Epifanio**Produtos naturais: atualidade, desafios e perspectivas**
Quim Nova, 25 (2002), pp. 45-61, 10.1590/S0100-40422002000800009

[2]

R.C. Dutra, M.M. Campos, A.R.S. Santos, J.B. Calixto**Medicinal plants in Brazil: pharmacological studies, drug discovery, challenges and perspectives**
Pharmacol. Res., 112 (2016), pp. 4-29, 10.1016/j.phrs.2016.01.021

[3]

P. Severino, M.H.A. Santana, S.M. Malmonge, E.B. Souto**Polímeros usados como sistemas de transporte de princípios ativos**
Polymeros, 21 (2011), pp. 361-368, 10.1590/S0104-14282011005000061

[4]

R.C.M. de Paula, J.F. Rodrigues**Composition and rheological properties of cashew tree gum, the exudate polysaccharide from *Anacardium occidentale* L**
Carbohydr. Polym., 26 (1995), pp. 177-181, 10.1016/0144-8617(95)00006-S

[5]

D.S. Torquato, M.L. Ferreira, G.C. Sá, E.S. Brito, G.A.S. Pinto, E.H.F. Azevedo**Evaluation of antimicrobial activity of cashew tree gum**
World J. Microbiol. Biotechnol., 20 (2004), pp. 505-507, 10.1023/B:WIBI.0000040407.90110.c5

[6]

T.S.L. Araújo, D.S. Costa, N.A. Sousa, L.K.M. Souza, S. de Araújo, A.P. Oliveira, F.B.M. Sousa, D.A. Silva, A.L.R. Barbosa, J.R.S.A. Leite, J.V.R. Medeiros**Antidiarrheal activity of cashew gum, a complex heteropolysaccharide extracted from exudate of *Anacardium occidentale* L. in rodents**

J. Ethnopharmacol., 174 (2015), pp. 299-307, 10.1016/j.jep.2015.08.020

[7]

D.P.B. da Silva, I.F. Florentino, L.K. da Silva Moreira, A.F. Brito, V.V. Carvalho, M.F. Rodrigues, G.A. Vasconcelos, B.G. Vaz, M.A. Pereira-Junior, K.F. Fernandes, E.A. Costa**Chemical characterization and pharmacological assessment of polysaccharide free, standardized cashew gum extract (*Anacardium occidentale* L.)**
J. Ethnopharmacol., 213 (2018), pp. 395-402, 10.1016/j.jep.2017.11.021

[8]

N.S. Carvalho, M.M. Silva, R.O. Silva, L.A.D. Nicolau, F.B.M. Sousa, S.R.B. Damasceno, D.A. Silva, A.L.R. Barbosa, J.R.S.A. Leite, J.V.R. Medeiros**Gastroprotective properties of cashew gum, a complex heteropolysaccharide of *Anacardium occidentale*, in naproxen-induced gastrointestinal damage in rats**
Drug Dev. Res., 76 (2015), pp. 143-151, 10.1002/ddr.21250

[9]

N.A.O. Pitombeira, J.G. Veras Neto, D.A. Silva, J.P.A. Feitosa, H.C.B. Paula, R.C.M. de Paula**Self-assembled nanoparticles of acetylated cashew gum: characterization and evaluation as potential drug carrier**
Carbohydr. Polym., 117 (2015), pp. 610-615, 10.1016/j.carbpol.2014.09.087

[10]

S.F.L. Dias, S.S. Nogueira, F. de França Dourado, M.A. Guimarães, N.A. de Oliveira Pitombeira, G.G. Gobbo, F.L. Primo, R.C.M. de Paula, J.P.A. Feitosa, A.C. Tedesco, L.C.C. Nunes, J.R.S.A. Leite, D.A. da Silva**Acetylated cashew gum-based nanoparticles for transdermal delivery of diclofenac diethyl amine**
Carbohydr. Polym., 143 (2016), pp. 254-261, 10.1016/j.carbpol.2016.02.004

[11]

J.M. Barbosa-Filho, M.R. Piuvezam, M.D. Moura, M.S. Silva, K.V.B. Lima, E.V.L. Da-Cunha, I.M. Fechine, O.S. Takemura**Anti-inflammatory activity of alkaloids: a twenty-century review**
Rev. Bras, 16 (2006), pp. 109-139, 10.1590/S0102-695X2006000100020

[12]

T.S. Castilhos, R.B. Giordani, A.T. Henriques, F.S. Menezes, J.Â.S. Zuanazzi**Avaliação in vitro das atividades antiinflamatória, antioxidante e antimicrobiana do alcalóide montanina**
Rev. Bras, 17 (2007), pp. 209-214, 10.1590/S0102-695X2007000200013

[13]

B. Özçelik, M. Kartal, I. Orhan**Cytotoxicity, antiviral and antimicrobial activities of alkaloids, flavonoids, and phenolic acids**

Pharm. Biol., 49 (2011), pp. 396-402, 10.3109/13880209.2010.519390

[14]

Q. Li, K.-X. Yang, Y.-L. Zhao, X.-J. Qin, X.-W. Yang, L. Liu, Y.-P. Liu, X.-D. Luo**Potent anti-inflammatory and analgesic steroidal alkaloids from *Veratrum taliense***

J. Ethnopharmacol., 179 (2016), pp. 274-279, 10.1016/j.jep.2015.12.059

[15]

S. Perviz, H. Khan, A. Pervaiz**Plant alkaloids as an emerging therapeutic alternative for the treatment of depression**

Front. Pharmacol., 7 (2016), 10.3389/fphar.2016.00028

[16]

L.M. Veras, M.A. Guimaraes, Y.D. Campelo, M.M. Vieira, C. Nascimento, D.F. Lima, L. Vasconcelos, E. Nakano, S.S. Kuckelhaus, M.C. Batista, J.R. Leite, J. Moraes**Activity of epiisopiloturine against *Schistosoma mansoni***

Curr. Med. Chem., 19 (2012), pp. 2051-2058, 10.2174/092986712800167347

[17]

V.G. Silva, R.O. Silva, S.R.B. Damasceno, N.S. Carvalho, R.S. Prudêncio, K.S. Aragão, M.A. Guimarães, S.A. Campos, L.M.C. Véras, M. Godejohann, J.R.S.A. Leite, A.L.R. Barbosa, J.-V.R. Medeiros**Anti-inflammatory and antinociceptive activity of epiisopiloturine, an imidazole alkaloid isolated from *Pilocarpus microphyllus***

J. Nat. Prod., 76 (2013), pp. 1071-1077, 10.1021/np400099m

[18]

L.A.D. Nicolau, N.S. Carvalho, D.M. Pacífico, L.T. Lucetti, K.S. Aragão, L.M.C. Véras, M.H.L.P. Souza, J.R.S.A. Leite, J.V.R. Medeiros**Epiisopiloturine hydrochloride, an imidazole alkaloid isolated from *Pilocarpus microphyllus* leaves, protects against naproxen-induced gastrointestinal damage in rats**

Biomed. Pharmacother., 87 (2017), pp. 188-195, 10.1016/j.biopha.2016.12.101

[19]

M.A. Guimarães, Y.D.M. Campelo, L.M.C. Véras, M.C. Colhone, D.F. Lima, P. Ciancaglini, S.S. Kuckelhaus, F.C.A. Lima, J. de Moraes, J.R. de S. A. Leite**Nanopharmaceutical approach of epiisopiloturine alkaloid carried in liposome system: preparation and in vitro schistosomicidal activity**

J. Nanosci. Nanotechnol., 14 (2014), pp. 4519-4528, 10.1166/jnn.2014.8248

[20]

K. Miladi, S. Sfar, H. Fessi, A. Elaissari**Enhancement of alendronate encapsulation in chitosan nanoparticles**
J. Drug Delivery Sci. Technol., 30 (2015), pp. 391-396, 10.1016/j.jddst.2015.04.007

[21]

M. Talelli, M. Iman, A.K. Varkouhi, C.J.F. Rijcken, R.M. Schiffelers, T. Etrych, K. Ulbrich, C.F. van Nostrum, T. Lammers, G. Storm, W.E. Hennink**Core-crosslinked polymeric micelles with controlled release of covalently entrapped doxorubicin**
Biomaterials, 31 (2010), pp. 7797-7804, 10.1016/j.biomaterials.2010.07.005

[22]

K. Letchford, H. Burt**A review of the formation and classification of amphiphilic block copolymer nanoparticulate structures: micelles, nanospheres, nanocapsules and polymersomes**
Eur. J. Pharm. Biopharm., 65 (2007), pp. 259-269, 10.1016/j.ejpb.2006.11.009

[23]

W. Park, S. Park, K. Na**Potential of self-organizing nanogel with acetylated chondroitin sulfate as an anti-cancer drug carrier**
Colloids Surf. B: Biointerfaces, 79 (2010), pp. 501-508, 10.1016/j.colsurfb.2010.05.025

[24]

A. Batagin-Neto, E.F. Oliveira, C.F.O. Graeff, F.C. Lavarda**Modelling polymers with side chains: MEH-PPV and P3HT**
Mol. Simul., 39 (2013), pp. 309-321, 10.1080/08927022.2012.724174

[25]

G. Schaftenaar, E. Vlieg, G. Vriend**Molden 2.0: quantum chemistry meets proteins**
J. Comput. Aided Mol. Des., 31 (2017), pp. 789-800, 10.1007/s10822-017-0042-5

[26]

J.J.P. Stewart, MOPAC2009**Stewart Computational Chemistry: Colorado Springs, USA** (2009)

[27]

L.M.C. Véras, V.R.R. Cunha, F.C.D.A. Lima, M.A. Guimarães, M.M. Vieira, Y.D.M. Campelo, V.Y. Sakai, D.F. Lima, P.S. Carvalho Jr, J.A. Ellena, P.R.P. Silva, L.C. Vasconcelos, M. Godejohann, H.M. Petrilli, V.R.L. Constantino, Y.P. Mascarenhas, J.R. de Souza de Almeida Leite**Industrial scale isolation, structural and spectroscopic characterization of**

epiisopiloturine from *Pilocarpus microphyllus* Stapf leaves: a promising alkaloid against schistosomiasis
PLoS One, 8 (2013), Article e66702, 10.1371/journal.pone.0066702

[28]
W. Kohn, L.J. Sham**Self-consistent equations including exchange and correlation effects**
Phys. Rev., 140 (1965), pp. A1133-A1138, 10.1103/PhysRev.140.A1133

[29]
C. Lee, W. Yang, R.G. Parr**Development of the Colle-Salvetti correlation-energy formula into a functional of the electron density**
Phys. Rev. B, 37 (1988), pp. 785-789, 10.1103/PhysRevB.37.785

[30]
M.J. Frisch, *et al.***Gaussian09 Revision A.1, Gaussian 09, Revis. A.02**
(2009)

[31]
I. Cesarino, R.P. Simões, F.C. Lavarda, A. Batagin-Neto**Electrochemical oxidation of sulfamethazine on a glassy carbon electrode modified with graphene and gold nanoparticles**
Electrochim. Acta (2016), 10.1016/j.electacta.2016.01.178

[32]
E.S. Bronze-Uhle, A. Batagin-Neto, F.C. Lavarda, C.F.O. Graeff**Ionizing radiation induced degradation of poly (2-methoxy-5-(2′-ethyl-hexyloxy)-1,4-phenylene vinylene) in solution**
J. Appl. Phys., 110 (2011), Article 073510, 10.1063/1.3644946

[33]
A. Batagin-Neto, E. Bronze-Uhle, M. Vismara, A. Assis, F. Castro, T. Geiger, F. Lavarda, C. Graeff**Gamma-ray dosimetric properties of conjugated polymers in solution**
Curr. Phys. Chem., 3 (2013), pp. 431-440, 10.2174/18779468113036660026

[34]
L.O. Mandú, A. Batagin-Neto**Chemical sensors based on N-substituted polyaniline derivatives: reactivity and adsorption studies via electronic structure calculations**
J. Mol. Model., 24 (2018), Article 157, 10.1007/s00894-018-3660-5

[35]
L.M. Martins, S. de Faria Vieira, G.B. Baldacim, B.A. Bregadiolli, J.C. Caraschi, A. Batagin-Neto, L.C. da Silva-Filho**Improved synthesis of tetraaryl-1,4-dihydropyrrolo[3,2-b] pyrroles a promising dye for organic electronic devices: an experimental and theoretical approach**
Dyes Pigments, 148 (2018), pp. 81-90, 10.1016/j.dyepig.2017.08.056

[36]

V.R.R. Cunha, F.C.D.A. Lima, V.Y. Sakai, L.M.C. Véras, J.R.S.A. Leite, H.M. Petrilli, V.R.L. Constantino**LAPONITE®-pilocarpine hybrid material: experimental and theoretical evaluation of pilocarpine conformation**

RSC Adv., 7 (2017), pp. 27290-27298, 10.1039/C7RA02017A

[37]

M.C. Portes, J. De Moraes, L.M.C. Véras, J.R. Leite, A.C. Mafud, Y.P. Mascarenhas, A.E.V. Luz, F.C.D.A. De Lima, R.R. Do Nascimento, H.M. Petrilli, P.L.S. Pinto, G. Althoff, A.M.D.C. Ferreira**Structural and spectroscopic characterization of epiisopiloturine-metal complexes, and anthelmintic activity vs *S. mansoni***

J. Coord. Chem. (2016), pp. 1-39, 10.1080/00958972.2016.1182162

[38]

M. Gaumet, A. Vargas, R. Gurny, F. Delie**Nanoparticles for drug delivery: the need for precision in reporting particle size parameters**

Eur. J. Pharm. Biopharm., 69 (2008), pp. 1-9, 10.1016/j.ejpb.2007.08.001

[39]

K. Na, T. Bum Lee, K.-H. Park, E.-K. Shin, Y.-B. Lee, H.-K. Choi**Self-assembled nanoparticles of hydrophobically-modified polysaccharide bearing vitamin H as a targeted anti-cancer drug delivery system**

Eur. J. Pharm. Sci., 18 (2003), pp. 165-173, 10.1016/S0928-0987(02)00257-9

[40]

S. Hornig, T. Heinze**Efficient approach to design stable water-dispersible nanoparticles of hydrophobic cellulose esters**

Biomacromolecules, 9 (2008), pp. 1487-1492, 10.1021/bm8000155

[41]

S. Galindo-Rodriguez, E. Allémann, H. Fessi, E. Doelker**Physicochemical parameters associated with nanoparticle formation in the salting-out, emulsification-diffusion, and nanoprecipitation methods**

Pharm. Res., 21 (2004), pp. 1428-1439, 10.1023/B:PHAM.0000036917.75634.be

[42]

U. Bilati, E. Allémann, E. Doelker**Development of a nanoprecipitation method intended for the entrapment of hydrophilic drugs into nanoparticles**

Eur. J. Pharm. Sci., 24 (2005), pp. 67-75, 10.1016/j.ejps.2004.09.011

[43]

H.L. Alvarado, G. Abrego, M.L. Garduño-Ramirez, B. Clares, A.C. Calpena, M.L. García**Design and optimization of oleanolic/ursolic acid-loaded nanoplatforms for ocular anti-inflammatory applications**
Nanomedicine, 11 (2015), pp. 521-530, 10.1016/j.nano.2015.01.004

[44]

C.E. Mora-Huertas, H. Fessi, A. Elaissari**Polymer-based nanocapsules for drug delivery**
Int. J. Pharm., 385 (2010), pp. 113-142, 10.1016/j.ijpharm.2009.10.018

[45]

C. Gomez-Gaete, N. Tsapis, M. Besnard, A. Bochot, E. Fattal**Encapsulation of dexamethasone into biodegradable polymeric nanoparticles**
Int. J. Pharm., 331 (2007), pp. 153-159, 10.1016/j.ijpharm.2006.11.028

[46]

S.R. Schaffazick, S.S. Guterres, L. de L. Freitas, A.R. Pohlmann**Caracterização e estabilidade físico-química de sistemas poliméricos nanoparticulados para administração de fármacos**
Quim Nova, 26 (2003), pp. 726-737, 10.1590/S0100-40422003000500017

[47]

S. Hornig, H. Bunjes, T. Heinze**Preparation and characterization of nanoparticles based on dextran–drug conjugates**
J. Colloid Interface Sci., 338 (2009), pp. 56-62, 10.1016/j.jcis.2009.05.025

[48]

J.L. de Oliveira, E.V.R. Campos, C.M. Gonçalves da Silva, T. Pasquoto, R. Lima, L.F. Fraceto**Solid lipid nanoparticles co-loaded with simazine and atrazine: preparation, characterization, and evaluation of herbicidal activity**
J. Agric. Food Chem., 63 (2015), pp. 422-432, 10.1021/jf5059045

[49]

V. Filipe, A. Hawe, W. Jiskoot**Critical evaluation of nanoparticle tracking analysis (NTA) by NanoSight for the measurement of nanoparticles and protein aggregates**
Pharm. Res., 27 (2010), pp. 796-810, 10.1007/s11095-010-0073-2

[50]

A.B.M.B. Santhosh Kumar, M. Ganesh Kumar, L. Suguna, T.P. Sastry**Pullulan acetate nanoparticles based delivery system for hydrophobic drug**
Int. J. Pharm. Bio. Sci., 3 (2012), pp. 24-32

[51]

N. Ahuja, O.P. Katare, B. Singh**Studies on dissolution enhancement and mathematical modeling of drug release of a poorly water-soluble drug using water-soluble carriers**
Eur. J. Pharm. Biopharm., 65 (2007), pp. 26-38, 10.1016/j.ejpb.2006.07.007

[52]

C.S. Brazel, N.A. Peppas**Modeling of drug release from swellable polymers**
Eur. J. Pharm. Biopharm., 49 (2000), pp. 47-58, 10.1016/S0939-6411(99)00058-2

[53]

S. Dash, P.N. Murthy, L. Nath, P. Chowdhury**Kinetic modeling on drug release from controlled drug delivery systems**
Acta Pol. Pharm., 67 (2010), pp. 217-223
http://www.ncbi.nlm.nih.gov/pubmed/20524422

[54]

R.W. Korsmeyer, R. Gurny, E. Doelker, P. Buri, N.A. Peppas**Mechanisms of solute release from porous hydrophilic polymers**
Int. J. Pharm., 15 (1983), pp. 25-35, 10.1016/0378-5173(83)90064-9

[55]

N.F.S. de Melo, R. Grillo, A.H. Rosa, L.F. Fraceto, N.L. Dias Filho, E. de Paula, D.R. de Araújo**Desenvolvimento e caracterização de nanocápsulas de poli (L-lactídeo) contendo benzocaína**
Quim Nova, 33 (2010), pp. 65-69, 10.1590/S0100-40422010000100013